



Polymetallic nodules from the Pacific manganese nodule belt : linking micro-structure and chemical speciation to biogeochemical environment

Experiment number:
EC-718

Beamline: ID21	Date of experiment: from: 04/02/2011 to: 08/02/2011	Date of report: 2-08-2012
Shifts: 12	Local contact(s): Dr Barbara Fayard	<i>Received at ESRF:</i>

Names and affiliations of applicants (* indicates experimentalists):

Aude Picard*, Max Planck Institute for Marine Microbiology, Biogeochemistry Department, Celsiusstr. 1, 28359 Bremen, Germany – Present address : Eberhard Karls University Tuebingen, Center for Applied Geoscience, Sigwartstr. 10, 72076 Tuebingen, Germany

Thomas Kuhn*, Bundesanstalt fuer Geowissenschaft und Rohstoffe, Stilleweg 2, 30655 Hannover, Germany

Anna Wegorzewski*, Bundesanstalt fuer Geowissenschaft und Rohstoffe, Stilleweg 2, 30655 Hannover, Germany

Report

We analyzed the distribution, mineralogy and speciation of Mn in marine polymetallic nodules recovered in the Pacific Ocean. Samples were prepared as thin sections and analyzed at beamline ID21 by μ -XRF and μ -XANES at the Mn K-edge to link microstructure and chemical speciation to sediment biogeochemistry.

Choice of samples and standards:

Samples for this study were recovered in the Clarion-Clipperton fracture zone within the so-called “Pacific manganese nodule belt” in the north-east equatorial Pacific Ocean. Three nodules and one crust were analyzed. Measurements in the nodules focused on the surface (in contact with seawater), the bottom side (in contact with sediment) and the rim (in contact with the sediment-water interface). As a comparison, a nodule collected in the Peru Basin was also analyzed. Rhodocrosite (MnCO_3), Mn-diaspore (MnOOH) and pyrolusite (MnO_2) were selected as references for Mn^{2+} , Mn^{3+} and Mn^{4+} , respectively. Other references, typical of manganese nodules (e.g. vernadite, todorokite), were also measured.

Conditions of measurements:

Micro-XRF and micro-XANES measurements were performed on beamline ID21. Mn reference compounds were prepared as a powder and spread over a sulfur-free tape. Thin sections (1x1 cm) of nodule samples were mounted between two ultralene® foils. The distribution of Mn in the nodule thin sections was imaged using the scanning X-ray microscope at ID21 beamline (Susini et al., 2002). Samples were scanned in the microscope

chamber under vacuum with a monochromatic beam focused by a Fresnel zone plate at a spot size of $0.25 \times 0.75 \mu\text{m}^2$ (VxH, FWHM). The microprobe intensity was 9.10^9 ph s^{-1} with a storage ring current of 200 mA. The Mn K α fluorescence line was excited with an energy of 6.7 keV and its intensity was recorded using a photodiode. The integration time per pixel was 100 ms. Maps of several hundreds of μm^2 were recorded. Mn K-edge XANES spectra were recorded from 6.52 to 6.7 keV in 485 points with 0.3 s counting time using a fixed exit double-crystal Si111 monochromator of energy resolution 0.75 eV at 6.6 keV. Reference spectra were measured on reference powders with a large beam (100 μm) in transmission mode with a photodiode. Due to the fragility of the samples, the thin sections of the nodules could not be prepared thin enough to perform measurements in the transmission mode. Micro-XANES measurements at the Mn K-edge were performed in the fluorescence mode on the thin sections of the nodule samples on selected spots covering a large range of Mn abundances. Three to four spectra were measured at one spot and averaged. The incident beam energy was calibrated using a foil of elemental Mn(0).

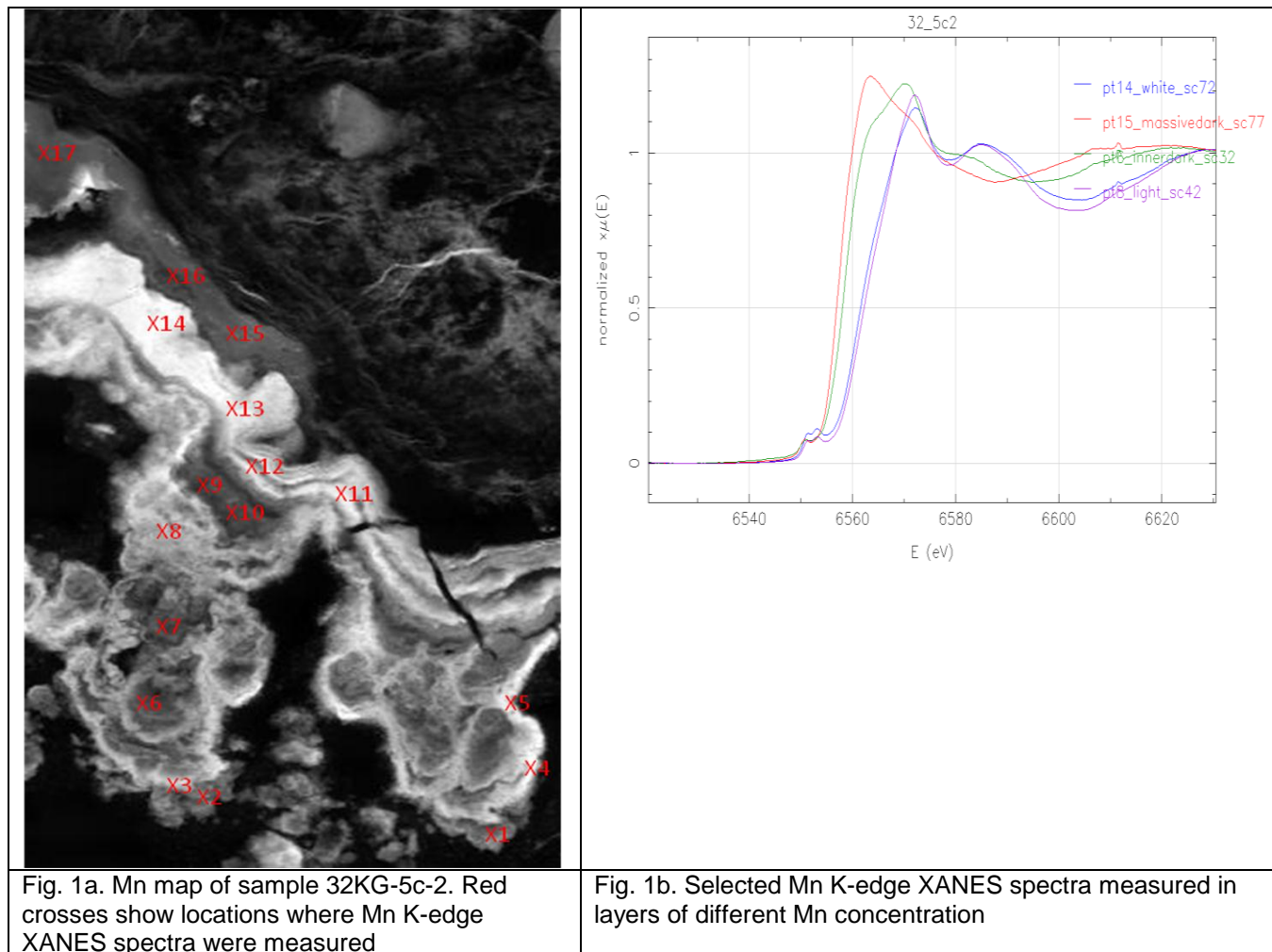
Data analysis:

XANES spectra were processed and analyzed using the Horae Athena free software (Newville, 2001 ; Ravel and Newville, 2005). Linear combination analyses were attempted to determine the mineralogical composition of the Mn minerals in the nodules. A pre-edge analysis of the Mn K-edge spectra was performed as described in Chalmin et al. (2009) using the free software Fityk (Wojdyr, 2010) to determine the local speciation of Mn in the nodule layers.

Results:

Five samples (4 nodules and 1 crust) were analyzed during the 12 shifts. Nodules consist of micro layers which are irregularly and concentrically banded around a nucleus (compressed sediment, fragment of igneous rock or older nodule). Micro-layers show different reflectivity under the optical microscope due to different chemical and mineralogical compositions. Light-colored layers usually show high Mn content (30-40 %wt) and low Fe content (1-3 %wt), as shown by microprobe analysis. Bulk XRD measurements revealed that Mn minerals in these layers consist of tectomanganate todorokite and phylломanganate birnessite. Mn minerals are of diagenetic origin (precipitation from the porewater) and the expected Mn redox state is between Mn³⁺ and Mn⁴⁺. In the dark-colored layers of the nodules, Mn is less abundant (20 %wt) and Fe is enriched (up to 23 %wt). Mn minerals form under hydrogenetic conditions (precipitation from the seawater under oxic conditions) and consist of vernadite intergrown with amorphous ferrihydrite and Mn redox state is expected to be Mn⁴⁺. **Measurements at ID21 were performed to bring information on the mineralogy and the Mn redox state in the Mn minerals at the sub-micron scale.** Figure 1a shows the Mn map of the bottom part of nodule 32KG-5c-2 sampled from a core box. Figure 1b shows selected Mn K-edge XANES spectra measured in layers of different Mn concentrations. The white layer on the map has a high Mn content. The analysis of the pre-edges of Mn K-edge XANES spectra measured in the white layer revealed an intermediate Mn redox between Mn³⁺ and Mn⁴⁺. However the linear combination analysis of the XANES spectra do not allow to distinguish between minerals (todorokite and birnessite). The dark layer on the map has a low Mn content. Macro-analyses suggest that the layer is of hydrogenetic formation, therefore vernadite is expected also at the micro-scale.

However the Mn K-edge XANES spectra measured in the dark layers are very different from the vernadite standard spectrum measured on the powder. Moreover the energy of the pre-edge of the spectra suggests that Mn is reduced (Mn^{2+}) which is not consistent with the macro analysis. Similar results have been obtained with the other nodules and the crust.



Conclusion:

It appears difficult to determine the exact mineralogy of Mn in the different layers of the nodules using the XANES spectra at the Mn K-edge (linear combination fitting). The analysis of the pre-edge centroid allows the determination of the Mn oxidation state in the Mn minerals. However discrepancies were observed between the bulk analysis of the nodules by XRD and the micro-analysis of the nodule layers. While Mn-rich layers (light-colored on the fluorescence maps) show a redox state of $\text{Mn}^{3+}/\text{Mn}^{4+}$, Mn-poor layers (dark-colored layers) apparently show a reduced state of Mn (Mn^{2+}). The Mn-poor layers have been shown to contain vernadite (Mn^{4+}). The Mn K-edge spectrum of the reference vernadite measured with a macro beam is consistent with the literature (e.g. Chalmin et al. 2009) while the spectra measured in the dark layers of the nodule and crust samples are very different from the reference and show a reduced oxidation state. It is possible that the “vernadite” component in the nodules get reduced under the conditions of the micro-beam used in the X-ray microscope. Other species such as MnO_2 were apparently stable under the beam. We have to test the stability of vernadite and other standards under the micro-beam.

References:

- Chalmin E., Farges F. and Brown Jr G.E. (2009). A pre-edge analysis of Mn K-edge XANES spectra to help determine the speciation of manganese in minerals and glasses. *Contrib. Mineral. Petrol.* 157: 111-126.
- Newville M. (2001) IFFEFIT: interactive XAFS analysis and FEFF fitting. *J. Synchrotron Radiat.* 8, 322-324.
- Ravel B. and Newville M. (2005) ATHENA, ARTEMIS, HEPHAESTUS: data analysis for X-ray absorption spectroscopy using IFFEFIT. *J. Synchrotron Radiat.* 12, 537-541.
- Susini J., Salomé M., Fayard B., Ortega R., Kaulich B. (2002) The scanning X-ray microprobe at the X-ray microscopy beamline at the ESRF, *Surf. Rev. Lett.* 9: 203-211.
- Wojdyr M. (2010) Fityk: a general-purpose peak fitting program. *J. Appl. Cryst.* 43: 1126-1128.